Benzodithiophene unit copolymerization to improve the stability of thiophene-based organic solar cells

Hiroki Saito[1], Takayuki Uchiyama[1], Yoshiko Okada-Shudo[1] Wendimagegne Mammo[2],Tjaart Kruger [3] Varun Vohra [1] Newayemedhin A. Tegegne[4*]

[1] Department of Engineering Science, The University of Electro-Communications, 1-5-1 Chofugaoka, Chofu City, 182-8585 Tokyo, Japan
[2] Department of Chemistry, Addis Ababa University, P.O.Box 33658 Addis Ababa, Ethiopia
[3] Department of Physics, University of Pretoria, Pretoria, South Africa
[4] Department of Physics, Addis Ababa University, P.O.Box 1176, Addis Ababa, Ethiopia

E-mail: newaye.medhin@aau.edu.et

August 2017

Abstract. With the increasing performance of organic solar cells (OSCs), the design of stable donor materials is of paramount importance. In this work, we synthesised a simple alternating copolymer with thiophene and BDT (P3T-BDT) units to understand the impact of incorporation of BDT on the thermal stability of the commonly used thiophene-based OSCs. OSCs fabricated with P3T-BDT:$PC_{71}BM$ and P3HT:$PC_{71}BM$ with 1:4 ratios displayed a different degradation kinetics despite their similar initial power conversion efficiency (PCE). The PCE of P3HT-based device degraded by half while the P3T-BDT-based device lost only 15% of its initial PCE after thermally being degraded at 85 °C for 48 h mainly due to the decrease in J_{sc}. Thermally-induced degradation of P3HT caused chain breakage while the P3T-BDT remained intact. The surface morphology of P3HT:$PC_{71}BM$ film exhibited a large increase in roughness in the first few hours leading to a loss of more 40% of its initial PCE while the P3T-BDT based OSC had a similar roughness throughout the accelerated ageing. This is also confirmed by the growth of the PL intensity of P3HT:$PC_{71}BM$ while P3T-BDT:$PC_{71}BM$ remained the same confirming a suppression of demixing of the donor and acceptor in the latter. In summary, the addition a BDT unit in the thiophene-based homopolymer was found to improve the thermal stability thiophene-based OSCs.

Keywords: Stability, Organic Solar cells, copolymerization, demixing and chain breakage

Submitted to: *J. Phys. D: Appl. Phys.*

1. Introduction

Until about a decade ago, thiophene homopolymers like poly(3-hexylthiophene) (P3HT) coupled with fullerene ($PC_{61}BM$) derivatives were considered to be the state-of-the-art electron donor and electron acceptor materials used in active layers organic solar cells (OSCs).[1] The power conversion efficiencies (PCEs) achieved with the P3HT:$PC_{61}BM$ active layers had relatively low values below 5% but progress in organic semiconductor design has enabled the fabrication of OSCs with PCEs as high as 19%.[2, 3] Because high PCE values are now commonly associated with non-fullerene acceptors, the essential role that the design and development of low band gap copolymers played to produce high efficiency OSCs is often overlooked.[4] However, replacing simple thiophene homopolymers like P3HT with low band gap copolymers composed of at least two alternating monomer units opened the path to OSCs that exhibit power conversion efficiencies (PCEs) above the milestone value of 10%.[5, 6, 7, 8] Copolymers like PTB7, PTB7-Th, PBDB-T and PM6, which are the new state-of-the-art electron donors in the OSC field, all employ benzodithiophene (BDT)-based monomers coupled with thiophene-based oligomers or thienothiophene (TT) units. [6, 7, 8, 9, 10, 11, 12]

Although incorporation of BDT units into copolymer designs clearly leads to large increases in the photovoltaic performance of OSCs, the impact of BDT addition on the stability of the resulting electron donors and on the durability of the corresponding OSCs is still very much under debate. P3HT-based OSCs are generally considered to be prone to facile degradation in air or through mild thermal stress, which explains why P3HT-based OSCs could not find commercial applications. The fast decrease in OSC performance observed for P3HT-based OSCs results from either oxidation of the thiophene rings or from demixing of the electron donor and electron acceptor in the OSC active layers.[13, 14, 15, 16, 17] Previous studies suggest that similar durability can be achieved for P3HT and PTB7-based OSCs under the adequate degradation conditions but that UV exposure accelerates the degradation of PTB7 OSCs.[18] Additionally, when employed in organic field effect transistors, PBDB-T exhibits enhanced stability with respect to P3HT. [19] However, results from other groups indicate that P3HT based OSCs are more stable than PTB7-Th ones.[20] Although these studies are essential to understand which materials have the highest potential when it comes to efficient and durable OSC manufacturing, the impact of BDT incorporation into the molecular structure on the OSC durability cannot be directly assessed by comparing P3HT with the aforementioned copolymers. PTB7 and PTB7-Th use BDT units combined with TT units and thus the differences in stability could be either due to the presence of BDT or to the fact that thiophene units were substituted with TT ones. Similarly, the complex molecular designs of PBDB-T and PM6 remove the possibility to directly understand the impact of BDT unit incorporation when comparing them with P3HT, a simple polymer composed of thiophene units and alkyl side chains.

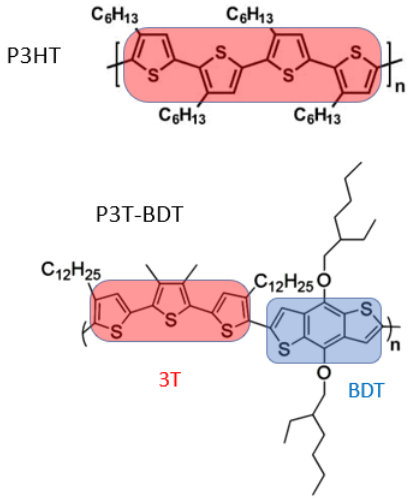

Figure 1: Molecular structures of P3HT and **P3T-BDT**.

In this study, we synthesize an alternating copolymer (P3T-BDT) composed of alkyl-substituted terthiophene (3T) units coupled with the simple 2-ethylhexyloxy-substituted BDT monomer present in PTB7 (Figure 1) and systematically compared the properties and degradation dynamics of P3T-BDT- and P3HT-based thin films and OSCs. We also analyzed the evolution of photovoltaic (PV) parameters in the OSCs, optical properties and crystallinity of the polymers as well as the oxidation dynamics in thin films and devices exposed to accelerated degradation conditions at 85 C. We found that the fast degradation observed in P3HT OSCs is essentially related to a fast decrease in short-circuit current density (J_{sc}). This decrease in J_{sc} can be mostly ascribed to P3HT crystallization-induced phase separation between P3HT and $PC_{71}BM$, which is avoided when using P3T-BDT instead of P3HT. P3T-BDT also exhibited slower oxidation dynamics compared to P3HT resulting in relatively stable J_{sc} values for up to 48 h at 85 °C. Our results thus provided a direct confirmation for the first time that BDT incorporation into the conjugated polymer backbone has positive impact on the material stability and device durability, which is an essential step towards the design of efficient and durable OSCs.

2. Result and Discussion

P3T-BDT was specifically designed to elucidate the impact of BDT addition on the stability of the electron donor and the durability of the OSCs rather than achieving high PCE values. Furthermore, a high concentration of $PC_{71}BM$ was employed in the blend active layers as this strategy generally slows the oxidation dynamics of the electron donor. [21] Because of the two aforementioned strategies, the P3HT and P3T-BDT OSCs produce relatively low initial average PCEs around 1.6% (Table 1). Nevertheless, all OSCs exhibited sufficiently high initial J_{sc} above 5 $mA.cm^{-2}$, thus ensuring the validity of our experiments and conclusions. The relatively low initial PV performances can be ascribed to the large acceptor concentration in the active layers which led to low fill factors (FF).

Despite the similar PV parameters initially produced by the two types of OSCs, P3HT and P3T-BDT OSCs exhibited very different PCE trends when exposed to accelerated degradation at 85 °C (Figure 2a). The PCE of P3HT OSCs quickly dropped to approximately 60% of its initial value within 1 h of annealing and then stabilizes to reach approximately half of its initial value after 48 h at 85 °C. On the other hand, after an initial increase, the PCE of P3T-BDT OSCs only decreased to around 85% of its initial value after 48 h at 85 °C. Note that the maximum PCE value for P3T-BDT OSCs (2.16%) is obtained after 1 h at 85 °C (see current density-voltage curves and PV parameters in Figure S1 and Table S1). A closer look of the evolution of each PV parameter, namely J_{sc}, the open-circuit voltage (V_{oc}), and the FF, was obtained by normalizing to their values acquired in the fresh samples in order to understand the reasons behind the difference in trends. The FF of both active layers maintained a relatively constant value with a mild decrease of less than 20% within the accelerated degradation period (Figure 2d). It should be emphasized here that after 24 h of annealing, the decrease in FF was slightly higher for P3T-BDT OSCs compared to those fabricated from P3HT. The V_{oc} of both OSCs display a notable increase of 20 - 30% within the first annealing hour, after which the values remained fairly constant up to 48 h of accelerated degradation. Unlike FF and V_{oc}, clear differences can be found in the initial J_{sc} variations for the P3HT:$PC_{71}BM$ active layers compared to the P3T-BDT:$PC_{71}BM$ ones. In fact, the PCE evolution over the studied period is governed by the trends in J_{sc} with slightly milder decreases in PCE values due to the 20- 30% increase in V_{oc} mentioned above. As PCE trends are mostly governed by the J_{sc} trends (Figure 2b), the following discussion focuses mainly on this PV parameter.

Electron Donor	J_{sc} (mA/cm^2)	V_{oc} (V)	FF (%)	PCE[a] (%)
P3HT	8.0	0.55	37.6	1.64
P3T-BDT	5.9	0.69	39.5	1.60

[a] averaged over 8 devices

Table 1: Average PV parameters of P3HT and P3T-BDT OSCs

Unlike the J_{sc} of the P3HT active layers, which quickly dropped to around half of its initial value, the maximum photocurrent produced by the P3T-BDT active layers increased by 10% after 1h of annealing. Note that the active layers were annealed at 120 °C for 10 min prior to electrode deposition to ensure that no solvent traces remained in the active layer. The difference in J_{sc} trends for the P3HT:$PC_{71}BM$ and P3T-BDT:$PC_{71}BM$ active layers can be ascribed to one of the two following deterioration mechanisms: (1) a thermally-induced decrease in absorbance leading to less efficient photon generation; (2) the formation of large donor and acceptor phase-separated domains upon annealing, which produce smaller donor-acceptor interface and thus decrease the charge separation efficiency. We should mention that a drop in absorbance generally corresponds to either the degradation of the intrinsic opto-electronic properties of the polymer chain (e.g., break in conjugation) or to changes in the crystalline order in the films. To understand whether the initial drop in J_{sc} of the P3HT active layers can be associated with a thermally-induced absorbance decrease, we measured the absorption spectra of the two polymers in their pristine states and after annealing them at 85 °C for 3 h and 24 h, respectively (Figure 3a). It should be noted that the absorbance of the two polymers did not change after being annealed for 1 h (data not shown for clarity), ruling out the assumption that absorbance contributed to the increase in J_{sc} of P3T-BDT based OSCs.

The two polymer thin films exhibited very similar spectral shapes in their pristine states. However, addition of BDT units to the thiophene backbone produced a bathochromic shift of the absorption maximum from 513 nm (P3HT) to 525 nm (P3T-BDT). Although P3HT exhibits changes in spectral shape and a decrease in absorbance upon exposure Previous studies have clearly demonstrated that crystallinity of P3HT can influence both the spectral shape of its absorption spectrum and the absorbance of its thin films.[22, 23] Therefore, we first verified whether the rapid decrease in absorption intensity from the P3HT films can be associated with changes in crystallinity of the films (Figures 3b). Clear crystallinity peaks can be observed in the diffraction

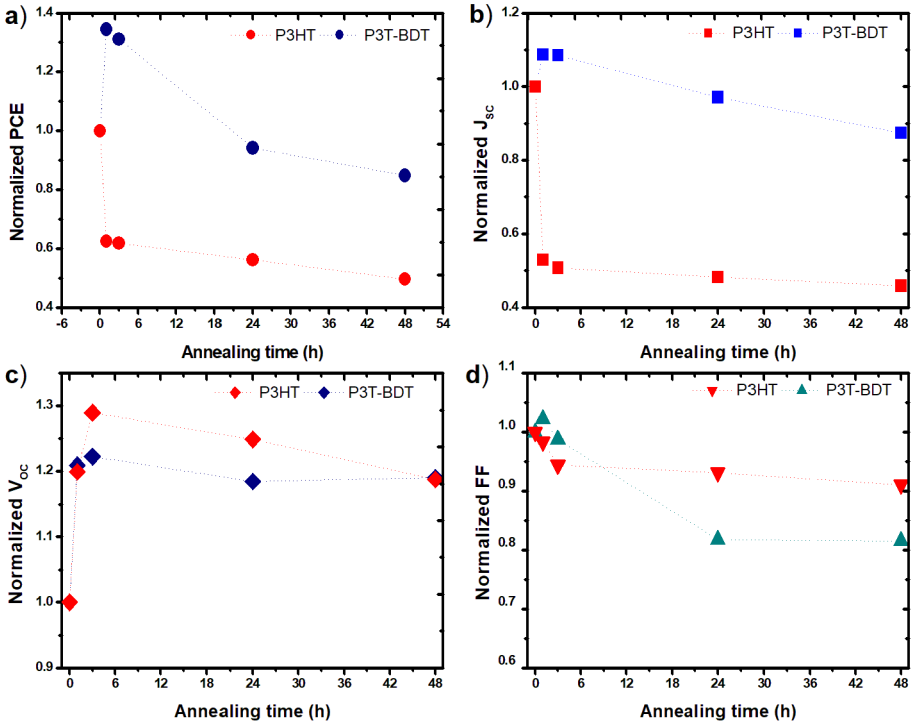

Figure 2: (a) Evolution of (a) the PCE b) J_{sc}, c)V_{oc} and d) FF of P3HT or P3T-BDT OSCs when annealed at 85 °C for up to 48 h.

patterns of P3HT films independently of the annealing conditions. However, a mild decrease in diffraction intensity is found for films annealed for 3 h and 24 h, respectively. After 24 h of annealing, the peak found around 5.2 degrees is reduced by approximately 9%, a much smaller reduction compared to that of the P3HT absorbance. The changes in P3HT spectral shape with larger relative contributions from the 0-0 vibronic transition around 610 nm also suggest that the origins of the absorbance loss in P3HT films may be related to lower crystallinity of the films. However, we cannot exclude the possibility that the lower absorbance is also partially caused by oxidation of the conjugated backbone resulting in breaks in conjugation.

On the other hand, Figure 3c clearly indicates that the crystalline order in the P3T-BDT thin films is much lower than in the P3HT ones. However, unlike P3HT thin films, the X-ray diffraction (XRD) patterns of the relatively amorphous P3T-BDT seem to maintain the same intensity even after annealing for 24 h. The minor decrease observed after 3 h of annealing could be caused by measurement error related to the low initial peak intensity. Together with the lack of notable decrease in P3T-BDT absorption intensity upon annealing, these results suggest that inclusion of BDT units into the thiophene backbone prevents breaks in conjugation length or other degradation mechanisms. The major P3HT degradation mechanisms, namely, oxidation of the conjugated backbone and side chains, have been previously studied using X-ray photoelectron spectroscopy (XPS).[15] Similarly, we investigated the properties of P3HT and P3T-BDT thin films by monitoring the changes in their C1s and S2p peaks upon annealing for 0 h, 3 h, 24 h and 1 week, respectively. Previous studies suggested that the carbon oxidation mechanism results in the formation of ester groups.[15] We could also observe the gradual formation of ester groups in the C1s spectra of P3HT thin films upon annealing. However, the decrease in the main C1s peak intensity at 284.9 eV and the increase in signal from the ester groups at 288.5 eV were very mild. In fact, clear formation of the ester groups could only be observed after 1 week of accelerated degradation at 85 °C. Note that degradation of the alkyl side chains of P3HT could also be responsible for a loss in crystallinity so these two causes for absorption intensity decrease may be interconnected. In contrast, the C1s spectra of P3T-BDT thin films exhibited minor changes even after 1 week of accelerated degradation, suggesting that the

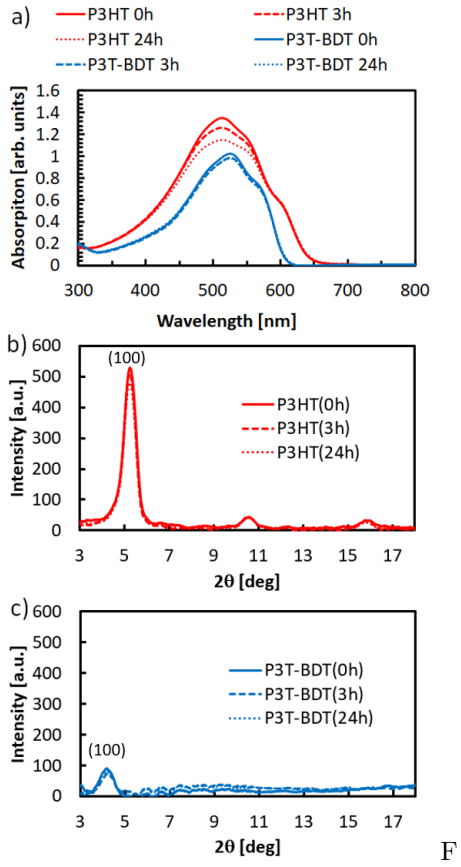

Figure 3: (a) absorption spectra of P3HT and P3T-BDT thin films in their pristine and annealed states; corresponding XRD patterns for (b) P3HT and (c) P3T-BDT films

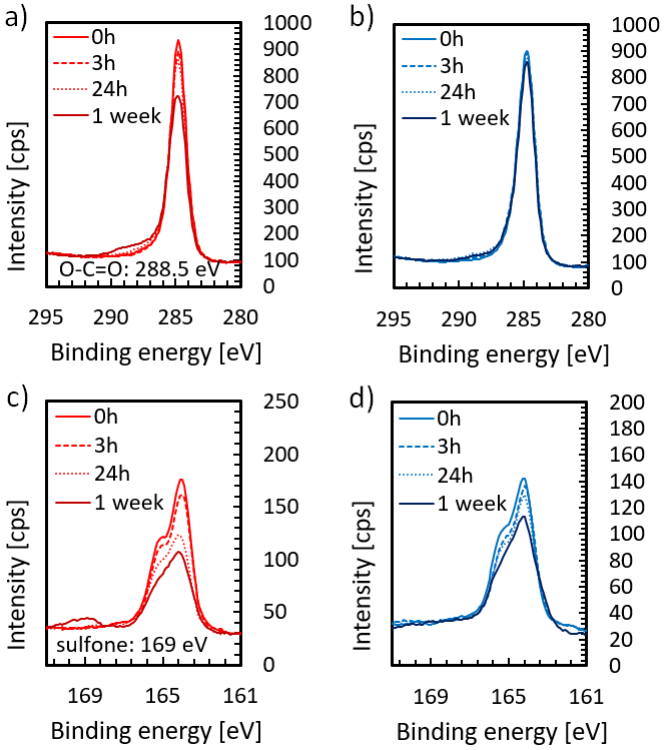

Figure 4: C1s spectra of (a) P3HT and (b) P3T-BDT thin films; S2p spectra of (c) P3HT and (d) P3T-BDT thin films.

presence of the BDT unit somehow hinders oxygen diffusion into the film or decreases its reactivity with the surrounding carbon atoms. Previous studies also revealed that sulfur oxidation results in thiophene ring opening, which causes major breaks in conjugation.[24] Despite the lower sulfur contents in the two polymers, clear decreases in S2p signal intensities upon annealing could be observed in the corresponding XPS spectra (Figure 4c and 4d). Nonetheless, similar to the C1s peak intensities, the dynamics of the intensity decrease for the S2p signal was much faster for P3HT compared to P3T-BDT. The peak intensity decrease observed in P3HT films after 3 h of annealing (- 11%) is similar to that observed in P3T-BDT films after 24 h of annealing.

Furthermore, after one week of annealing the P3HT films at 85 °C, a broad peak could be observed around 169 eV, which can be ascribed to the formation of sulfone species. [15] As these sulfone species can act as initiator for the thiophene ring opening degradation mechanism, avoiding their formation is an important step towards the manufacturing of long-lasting OSCs. The faster photo-bleaching rate and oxidation dynamics of P3HT correlate well with the overall J_{sc} and photovoltaic performance trends compared to P3T-BDT. However, as the P3HT absorption intensity only decreased by 6.7% after 3 h of annealing, other causes are likely involved in the abrupt J_{sc} decrease observed during the initial degradation of P3HT:PC_{71}BM OSCs. In particular, annealing induced phase separation can cause large notable changes in the electron donor and electron acceptor domain sizes sometimes resulting in large decreases in donor/acceptor interface.[25] To investigate changes in domain sizes as possible cause for the differences in J_{sc} trends, we started by monitoring the surface topography of P3HT:PC_{71}BM and P3T-BDT:PC_{71}BM active layers upon annealing for 3 h and 24 h at 85 °C using atomic force microscopy (AFM) images (Figure 5). First, the AFM images of pristine active layers suggested that more phase separation occurred in the pristine P3T-BDT:PC_{71}BM blends with respect to the P3HT:PC_{71}BM ones. This agrees with the difference in initial J_{sc} values observed for the two types of OSCs, wherein P3HT-based devices exhibited a J_{sc} value approximately 35% higher than that of P3T-BDT OSCs (Table 1). However, upon annealing for 3 h, the relatively flat

P3HT:$PC_{71}BM$ pristine films exhibit a large increase in surface roughness confirming that larger phase-separated domains could be formed during the initial degradation period.

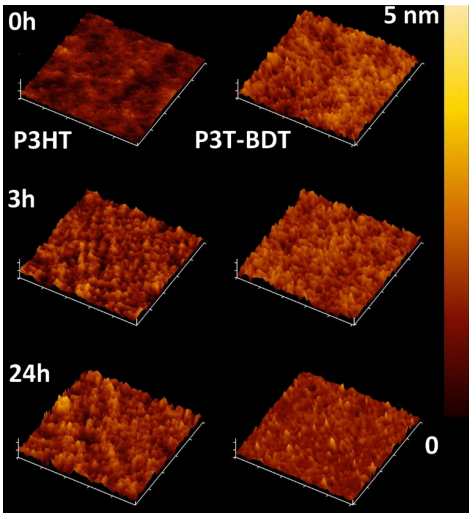

Figure 5: AFM images of P3HT:$PC_{71}BM$ and P3T-BDT:$PC_{71}BM$ active layers upon annealing for 3 h and 24 h at 85 ∘C.

After this initial degradation period, the P3HT:$PC_{71}BM$ active layer topography remains essentially the same for longer annealing times (e.g., 24 h). In contrast, the P3T-BDT:$PC_{71}BM$ blends, which initially exhibited a rather rough surface, maintain a similar roughness during the initial annealing period and seem to even become smoother at longer annealing times. Such differences are generally associated with miscibility of the donor and the acceptor in the OSC active layers.[26] Miscibility of the two materials can be quantitatively estimated using their surface free energies (s), which can be calculated from contact angle measurements using the Owens, Wendt, Rabel and Kaelble (OWRK) method.[27, 28] Similar s values do not necessarily result in highly miscible materials because s corresponds to the sum of its dispersive (sd) and polar (sp) components. Matching both these components is essential to have a high miscibility between the donor and the acceptor materials. Here, the sd and sp values for $PC_{71}BM$ were found to be 6.35 $mJ.m^{-2}$ and 13.14 $mJ.m^{-2}$, respectively, resulting in a s of 19.49 $mJ.m^{-2}$. The sp/s ratio for $PC_{71}BM$ thus has a value of 0.67, which is in good agreement with the values found in literature for the C60 PCBM derivative (sp/s = 0.73), which possesses a similar chemical structure to $PC_{71}BM$.[29] P3HT and P3T-BDT have much higher s values of 30.64 $mJ.m^{-2}$ and 32.14 $mJ.m^{-2}$, respectively. They also both exhibited similar sp/s values well below 0.01, confirming the apolar nature of the electron donors. The aforementioned values indicate that a better mixing should be obtained in pristine P3HT:$PC_{71}BM$ active layers compared to P3T-BDT:$PC_{71}BM$ ones which is consistent with the higher J_{sc} value and smoother surface obtained for pristine P3HT:$PC_{71}BM$ active layers with respect to P3T-BDT:$PC_{71}BM$ ones. The higher compatibility of $PC_{71}BM$ with P3HT would suggest less detrimental phase separation but the miscibility of $PC_{71}BM$ with the two donors may vary with annealing time and crystallinity. Unfortunately, since thermal energy induces changes in surface roughness, precise values could not be obtained for s, sd and sp values after annealing.

Phase separation in P3HT:$PC_{71}BM$ blends is often associated with crystallization of P3HT. Even though P3HT only films exhibit a decrease in crystalline order upon annealing (Figure 3), the crystallization dynamics in the blend films may differ. In fact, in their pristine state, P3HT:$PC_{71}BM$ thin films display a much lower crystalline order than P3HT only films and exhibited a broad and less intense diffraction peak (Figure 6a). In fact, unlike pristine P3HT thin films, the only peak that can be detected in the pristine blends corresponds to the lamellar (100) planes. Upon annealing P3HT:$PC_{71}BM$ thin films, crystalline order slightly improves which is translated as a narrowing of the (100) peak as well as an increase in peak intensity and the appearance of the (low intensity) second and third order peaks around 10.6 degrees and 15.8 degrees, respectively. The sudden narrowing of the (100) peak and the appearance of the second and third orders of diffraction indicate a denser packing of the P3HT crystallites, which should induce a demixing of P3HT and $PC_{71}BM$ molecules. On the other hand, the P3T-BDT crystalline peak can barely be detected in the pristine P3T-BDT:$PC_{71}BM$ blends and the blends remain relatively amorphous even upon annealing at 85 °C for 24 h (Figure 6b). Strong demixing between the electron donor and the electron acceptor, which would result in larger donor and acceptor domains, can be probed using photoluminescence (PL) quenching measurements. As the OSC active layers we investigated here contain a large amount of $PC_{71}BM$, we focused on the PL of the acceptor. A clear and intense PL peak can be observed from the pure $PC_{71}BM$ films excited at 470 nm (Figure 6c). Note that there is also a non-negligible amount of light absorption by the polymers at this excitation wavelength, but 470 nm corresponds to the best condition to clearly observe the $PC_{71}BM$ PL peak. The PL spectra of pure $PC_{71}BM$ films and blends were normalized to the $PC_{71}BM$ contents (thickness x $PC_{71}BM$ weight% in the films) in the samples. After 3 h of annealing at 85 °C, we can clearly observe a notable increase in PL of the P3HT:$PC_{71}BM$ blends. Assuming that the initial PL quenching ratio is

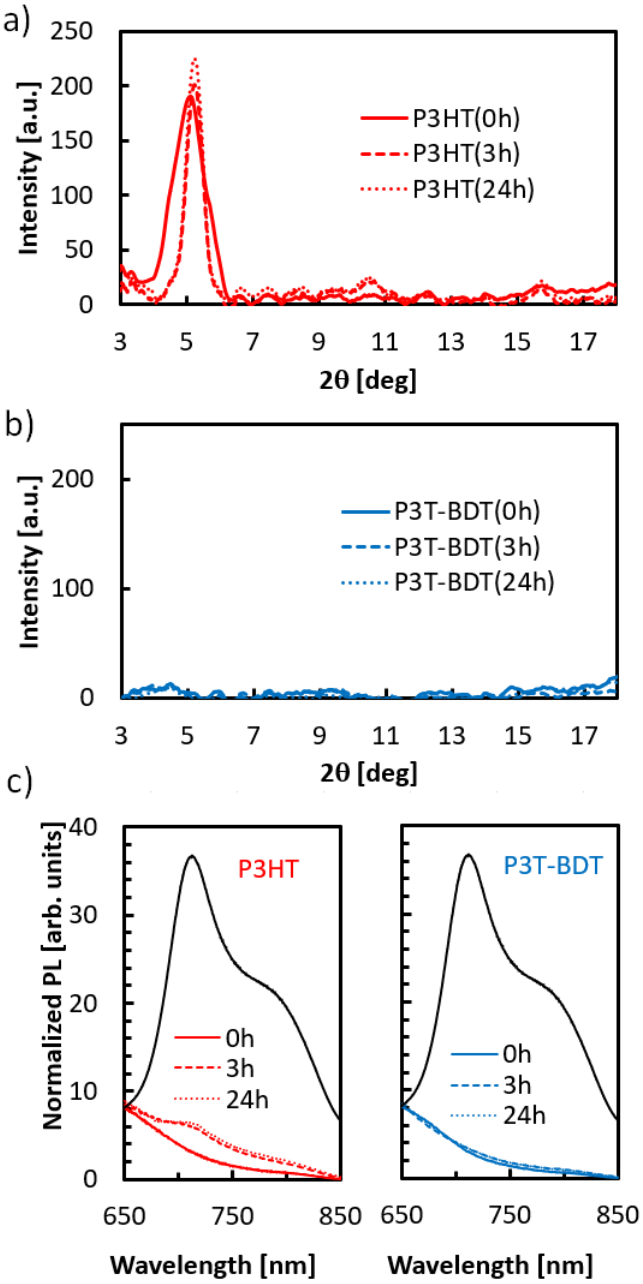

Figure 6: XRD pattern of (a) P3HT:$PC_{71}BM$ and (b) P3T-BDT:$PC_{71}BM$ thin films in their pristine and annealed states; and (c) their PL spectra when excited at 470 nm. The black lines correspond to the PL spectra of pure $PC_{71}BM$ thin films. All the PL spectra were normalized to the amount of $PC_{71}BM$ they contain.

100%, after 3 h and 24 h of thermal annealing, the PL quenching ratio decreased to 91 and 90%, respectively. These results are consistent with the AFM images in Figure 5, which suggest that larger donor and acceptor domains are formed after 3 h of annealing and that additional annealing does not considerably change the morphology of the P3HT:$PC_{71}BM$ blends. The PL spectra of P3T-BDT:$PC_{71}BM$ blends (Figure 6c) also confirm that no remarkable demixing is found in this binary system even when annealing the samples at 85 °C for 24 h. Note that similar trends in polymer PL quenching are expected in the two systems but the significant absorption by $PC_{71}BM$ at the excitation wavelengths for the polymers and the large relative concentration of $PC_{71}BM$ in the blends makes the analysis of the polymer PL quenching ratios highly inaccurate. Nevertheless, the $PC_{71}BM$ PL quenching ratios provide sufficient evidence to conclude that the lower PV performance stability observed in P3HT OSCs with respect to P3T-BDT ones is not solely related to loss of intrinsic optical properties of P3HT as a result of its faster oxidation dynamics but also due to the formation of large donor and acceptor domains from the thermally induced P3HT crystallization in the P3HT:$PC_{71}BM$ blend films.

3. Experimental

3.1. Synthesis of P3T-BDT

5,5”-Dibromo-4,4”-didodecyl-3’,4-dimethyl-2,2’:5’,2”-terthiophene (6) (193 mg, 0.25 mmol) and 2,6-bis(trimethyl-stannyl)-4,8-bis(2-ethylhexyloxy)benzo[1,2-b;4,5- b] dithiophene (7) (194 mg, 0.25 mmol) were placed in round-bottomed flask (25 mL). After introducing dry toluene (5 mL), the mixture was purged successively with vacuum/nitrogen cycles two times and then Pd2(dba)3 (7 mg, 0.01 mmol) and P(o-tol)3 (12 mg, 0.04 mmol) were added. The mixture was degassed and refilled with nitrogen once more and heated at 100 °C with stirring for 6.5 h. The reaction mixture was cooled to room temperature, the polymer was precipitated from MeOH and collected by filtration. The solid was dissolved in CHCl3 and washed with sodium diethyldithiocarbamate trihydrate overnight, and then with distilled water. The organic layer was separated and concentrated to small volume and the polymer was precipitated from MeOH and collected by filtration. The crude polymer was further purified by Soxhlet extraction with hexane, diethyl ether and CHCl3. The CHCl3 extract was concentrated, and the polymer was precipitated from MeOH, filtered and dried in vacuum oven at 40 °C for 16 h to give P3T-BDT (0.26 g, 98.4%) as dark-red solid. Mn = 59,100 g/mol, Mw = 149,200 g/mol. The synthesis scheme of the monomer (6) and the copolymer are given in Scheme S1 and S2, receptively.

3.2. Electrochemistry

The square-wave voltammetry measurement of P3T-BDT was performed on a BASi Epsilon-EC potentio-

stat. A three-electrode setup was used, with platinum disk as working electrode, platinum wire as counter electrode, and a Ag/Ag+ quasi-reference electrode. A 0.1 M solution of tetrabutylammonium perchlorate (TBAP) in anhydrous acetonitrile was used as supporting electrolyte. Thin polymer films were cast from CHCl3 solution onto the working electrode. Nitrogen was bubbled in to the electrolyte solution prior to each experiment. During the scans, nitrogen was flushed over the electrolyte surface. The platinum disk was polished by using 0.5 and 0.3 mm Al2O3 slurry followed by thoroughly rinsing with deionized water, and acetonitrile for each experiment. The potential of the quasi-reference electrode was corrected to the Ag/AgCl reference electrode by measuring the ferric/ ferrous (FeIII/FcII) redox couple in the supporting electrolytesolvent system, which was found to be 0.1 V versus Ag/AgCl. All potentials were reported in volts against the Ag/AgCl reference electrode. The HOMO and LUMO energy levels of P3T-BDT were deduced from its respective ionization potentials and electron affinities, estimated from the oxidation and reduction onset potentials according to the formulae $E_{HOMO/LUMO} = -(E_{ox/red} + 4.4)$ eV (see Figure S2).

3.3. Thin film and OSCs fabrication and Characterizations

The OSCs presented in this work were prepared in an inverted geometry of glass/indium-doped tin oxide (ITO)/Active layer/ molybdenum trioxide (MoO3)/silver/(Ag). The ITO-coated glass substrates were cleaned in the standard cleaning process with ultrasonication with acetone, detergent, deionized water, and isopropanol successively, each for 10 min, followed by exposure to isopropanol vapour to remove potential solvent traces. A mixture of 500 mg of ZnOAc.H2O and 101.4 mg of 2-aminoethanol in 5 mL of 2-methoxyethanol was spin coated on the precleaned ITO substrates at 3000 rpm for 40 s. This layer was annealed at 200 °C for 30 min and slowly cooled to room temperature to from a 30 nm thick ZnO layer. The active layer solutions were prepared in 1:4 (polymer:$PC_{71}BM$) ratio at a concentration of 50 mg/mL in o-DCB. The active layers were dried at 120 °C to remove all solvent traces before thermally evaporating MoO3 (8 nm) and Ag (70 nm) consecutively at low pressure conditions. The photovoltaic performances of the fabricated OSCs were measured in air using Keithley 2401 source meter under am AM 1.5 simulated solar irradiation with a power intensity of 100 mW/cm^2.

The thin films in this study were prepared under similar condition as the active layer of the OSCs. The photoluminescence and absorption of the pristine polymer and the polymer:$PC_{71}BM$ films were recorded using a PerkinElmer LS45 spectroflourometer and Edinburgh Instruments D-5 spectrophotometer, respectively. The morphologies of the active layer of the OSCs were investigated using atomic force microscopy (AFM) model NT-MDT NTEGRA in a tapping mode. The crystallographic property of both the pristine and blend films were determined using Shimadzu Scientific Instruments X-ray diffractometer-7000S fitted with Cu-Ka radiation and gun power of 40 kV × 40 mA.

3.4. Ageing

The accelerated thermal degradation of both the devices and the films were monitored by annealing the samples at 85 °C according to the ASTM 1171E requirements. [30] All the degradation studies were recorded by periodically taking the measurements and putting the samples back for further annealing.

Conclusion

An alternating copolymer, P3T-BDT was synthesized to investigate the impact of addition of BDT unit on the thermal stability of thiophene-based polymers, specifically P3HT. The OSCs prepared by blending the polymer:$PC_{71}BM$ (1:4) revealed a different degradation kinetics despite their similar initial PCE. The P3HT:$PC_{71}BM$-based OSC lost more than 40% of its initial PCE in the first 3 h of annealing at 85 °C , followed by a quick drop to 50% in 48 h while P3T-BDT:$PC_{71}BM$ lost only 15% in 48 h accelerated degradation time. The main reason for the evolution of the PCE was due to the trends in J_{sc} which was due to the loss in absorbance and demixing of the donor and acceptor in the active layers. In regard to the absorption, P3HT exhibited an absorbance loss of 15.2% together with a change in its absorption profile while P3T-BDT lost only 4.1% and kept its absorption profile after 48 h of annealing. This was attributed to both oxidation and loss of crystallinity of P3HT which was suppressed in P3T-BDT. In addition, the roughness of the active layer morphology of P3HT:$PC_{71}BM$ increased in the first 3 h confirming the evolution of a large phase-separated domains which reduced the exciton quenching. On the contrary, the P3T-BDT:$PC_{71}BMPC_{71}BM$ based active layer revealed a rough surface morphology before annealing and remained almost the same with a slight improvement thereby keeping its exciton quenching the same. The main reason for the evolution of the morphology of the devices was found to be thermally-induced crystallization of the P3HT leading to demixing of the donor and acceptor phases which was effectively suppressed in P3T-BDT-based OSCs.

Authors Contribution

The work was designed by VV, NT and WM. WM Synthesised and characterized the polymer, the rest of the measurements were done by HS and YO. We all contributed equally on the discussion and write up of the manuscript

Conflicts of Interests

The authors declare that they have no known competing financial interests or personal relationships that could have appeared to influence the work reported in this paper.

Acknowledgement

NT would like to acknowledge the support from Organization for Women in Science for the Developing World (OWSD). WM would like to acknowledge the financial support from the International Science Program (ISP), Uppsala University, Sweden.

References

[1] Dang M T, Hirsch L and Wantz G 2011 *Advanced Materials* **23** 3597–3602
[2] Ma W, Yang C, Gong X, Lee K and Heeger A J 2005 *Advanced functional materials* **15** 1617–1622
[3] Cui Y, Xu Y, Yao H, Bi P, Hong L, Zhang J, Zu Y, Zhang T, Qin J, Ren J *et al.* 2021 *Advanced Materials* **33** 2102420
[4] Meredith P, Li W and Armin A 2020 *Advanced Energy Materials* **10** 2001788
[5] Vohra V, Kawashima K, Kakara T, Koganezawa T, Osaka I, Takimiya K and Murata H 2015 *Nature Photonics* **9** 403–408
[6] Nam S, Seo J, Woo S, Kim W H, Kim H, Bradley D D and Kim Y 2015 *Nature Communications* **6** 1–9
[7] Nam S, Seo J, Han H, Kim H, Hahm S G, Ree M, Gal Y S, Anthopoulos T D, Bradley D D and Kim Y 2016 *Advanced Materials Interfaces* **3** 1600415
[8] Qin Y, Uddin M A, Chen Y, Jang B, Zhao K, Zheng Z, Yu R, Shin T J, Woo H Y and Hou J 2016 *Advanced Materials* **28** 9416–9422
[9] He Z, Zhong C, Su S, Xu M, Wu H and Cao Y 2012 *Nature Photonics* **6** 591–595
[10] He Z, Zhong C, Huang X, Wong W Y, Wu H, Chen L, Su S and Cao Y 2011 *Advanced Materials* **23** 4636–4643
[11] Zhang S, Qin Y, Zhu J and Hou J 2018 *Advanced Materials* **30** 1800868
[12] Yuan J, Zhang Y, Zhou L, Zhang G, Yip H L, Lau T K, Lu X, Zhu C, Peng H, Johnson P A *et al.* 2019 *Joule* **3** 1140–1151
[13] Duan L and Uddin A 2020 *Advanced Science* **7** 1903259
[14] Hintz H, Peisert H, Egelhaaf H J and Chassé T 2011 *The Journal of Physical Chemistry C* **115** 13373–13376
[15] Manceau M, Gaume J, Rivaton A, Gardette J L, Monier G and Bideux L 2010 *Thin Solid Films* **518** 7113–7118
[16] Motaung D E, Malgas G F, Nkosi S S, Mhlongo G H, Mwakikunga B W, Malwela T, Arendse C J, Muller T F and Cummings F R 2013 *Journal of Materials Science* **48** 1763–1778
[17] Malgas G F, Motaung D E and Arendse C J 2012 *Journal of Materials Science* **47** 4282–4289
[18] Bartesaghi D, Ye G, Chiechi R C and Koster L J A 2016 *Advanced Energy Materials* **6** 1502338
[19] Brixi S, Melville O A, Boileau N T and Lessard B H 2018 *Journal of Materials Chemistry C* **6** 11972–11979
[20] Tyagi P, Hua S C, Amorim D R, Faria R, Kettle J and Horie M 2018 *Organic Electronics* **55** 146–156
[21] Uchiyama T, Sano T, Okada-Shudo Y and Vohra V 2020 *Journal of Materials Chemistry C* **8** 7162–7169
[22] Rahimi K, Botiz I, Agumba J O, Motamen S, Stingelin N and Reiter G 2014 *RSC Advances* **4** 11121–11123
[23] Kadem B Y, Al-hashimi M K and Hassan A 2014 *Energy Procedia* **50** 237–245
[24] Sai N, Leung K, Zádor J and Henkelman G 2014 *Physical Chemistry Chemical Physics* **16** 8092–8099
[25] Han J, Bao F, Huang D, Wang X, Yang C, Yang R, Jian X, Wang J, Bao X and Chu J 2020 *Advanced Functional Materials* **30** 2003654
[26] Ye L, Collins B A, Jiao X, Zhao J, Yan H and Ade H 2018 *Advanced Energy Materials* **8** 1703058
[27] Kaelble D 1970 *The Journal of Adhesion* **2** 66–81
[28] Owens D K and Wendt R 1969 *Journal of Applied Polymer Science* **13** 1741–1747
[29] Perrin L, Nourdine A, Planes E, Carrot C, Alberola N and Flandin L 2013 *Journal of Polymer Science Part B: Polymer Physics* **51** 291–302
[30] ASTM *American standard testing of Material* **1171E**